Electronic correlations in the superconductor $LaFeAsO_{0.89}F_{0.11}$ with low carrier density

Athena S. Sefat, Michael A. McGuire, Brian C. Sales, Rongying Jin, Jane Y. Howe, and David Mandrus
Materials Science and Technology Division, Oak Ridge National Laboratory, Oak Ridge, Tennessee 37831, USA
(Received 13 March 2008; revised manuscript received 3 April 2008; published 5 May 2008)

The crystal structure and numerous normal and superconducting state properties of layered tetragonal ($P4/nmm$) LaFeAsO, with F doping of $\approx 11\%$, are reported. Resistivity measurements give an onset transition temperature $T_c = 28.2$ K, and low field magnetic susceptibility data indicate bulk superconductivity. In applied magnetic field, analysis of the resistive transition results in a critical field $H_{c2} \approx 30$ T and a coherence length $\xi_{GL} \approx 35$ Å. An upper limit for the electron carrier concentration of 1×10^{21} cm^{-3} is inferred from the Hall data just above T_c. Strong electron-electron correlations are suggested from temperature-dependent resistivity, Seebeck coefficient, and thermal conductivity data. Anomalies near T_c are observed in both Seebeck coefficient and thermal conductivity data.

DOI: 10.1103/PhysRevB.77.174503 PACS number(s): 74.70.−b, 74.72.−h, 75.30.Cr, 61.05.C−

I. INTRODUCTION

Recently, an oxide family of layered tetragonal superconductors containing the transition metal elements Fe and Ni has been reported: LaFePO ($T_c = 4$ K, increasing to $T_c \sim 7$ K with F doping),[1,2] LaNiPO ($T_c = 3$ K),[3] and LaFeAsO ($T_c = 26$ K at 5%–11% F doping).[4] These quaternary compounds crystallize with the ZrCuSiAs-type structure[5] in $P4/nmm$ space group (No. 129; $Z=2$).[6,7] Recent electronic structure calculations[8] describe the structure as sheets of metallic Fe^{2+} in between ionic blocks of $LaOAs^{2-}$. Although there is bonding between Fe and As ($d = 2.3$–2.4 Å), the states near the Fermi level are dominated by Fe d states lightly mixed with As p states. A view of the structure emphasizing this viewpoint is shown in Fig. 1(a). La atoms (with $4mm$ site symmetry) are coordinated by four As and four O atoms, forming distorted square antiprisms. The Fe atoms ($\bar{4}2m$) form square nets perpendicular to the c-crystallographic direction.

The focus of this study is the $LaFeAsO_{1-x}F_x$ system with nominal composition of $x \approx 0.11$.[4,9,10] The large reported T_c of approximately 26 K in this compound is very exciting because of the similarities between this layered transition metal compound and the high T_c cuprates. Its discovery may lead to related superconducting compounds with potentially higher T_c's, but may also provide insight into superconductivity in layered transition metal oxides. The experimental details below are followed by a discussion of the $LaFeAsO_{0.89}F_{0.11}$ crystal structure. The thermodynamic and transport properties of this material will then be presented and discussed. The measurements include temperature-dependent Hall effect, field- and temperature-dependent magnetic susceptibility, electrical resistivity, Seebeck coefficient, and thermal conductivity.

II. EXPERIMENTAL DETAILS

Polycrystalline samples with $LaFeAsO_{0.89}F_{0.11}$ nominal composition were prepared by a standard solid-state synthesis method similar to that reported by Kamihara *et al.*[4] First, LaAs was prepared by placing mixtures of La (purity 99.9%) and As (99.999%) in a silica tube. The La and As pieces were slowly reacted by heating from 600 to 700 °C (1 °C/min, dwell for 24 h), then to 900 °C (1 °C/min, dwell for 30 h), and finally to 950 °C (1 °C/min, dwell for 20 h). $LaFeAsO_{0.89}F_{0.11}$ were synthesized by stoichiometrically mixing fine powders of LaAs, Fe_2As (99.5%), La_2O_3 (99.99%, calcined at 900 °C for 12 h), LaF_3 (99.99%), As (99.999%), pressing into a pellet, and rapidly heating in a silica tube. The silica was partially filled with high purity Ar gas and heated at 1250 °C for ~15 h, then rapidly cooled by shutting off the furnace. The pellet was reground and reannealed at 1250 °C. The source of all elements or compounds was Alpha Aesar.

The phase purity and structural identification were made via powder x-ray diffraction by using a Scintag XDS 2000 θ-θ diffractometer (Cu $K\alpha$ radiation). Data for Rietveld[11] refinement were collected over a 2θ range of 15°–120° with a step size of 0.02° and a counting time of 10 s/step. The data were refined with main phase of $LaFeAsO_{0.89}F_{0.11}$ (Ref. 4) and small impurity phase of $La_{4.67}(SiO_4)_3O$.[12] Refined parameters include zero point offset, ten background polynomial coefficients, two asymmetry parameters, scale factors, preferred orientation, shape and half-width parameters, lattice constants, the two variable atomic positions in $LaFeAsO_{0.89}F_{0.11}$ (z coordinates for La and As), and overall isotropic displacement parameters. As expected, the fit was relatively insensitive to the O:F ratio, which was fixed at the nominal value for the final refinement cycles. Atomic positions of the lanthanum silicate oxide phase were not refined but fixed at the literature values.

Electron probe microanalysis of a polished surface of the polycrystalline pellet was performed on a JEOL JSM-840 scanning electron microscope (SEM) by using an accelerating voltage of 10 kV and a current of 20 nA with an energy-dispersive x-ray analysis brand energy-dispersive spectroscopy device attached to the SEM. Transmission electron microscopy (TEM) data were collected on a Hitachi HF-3300 TEM/scanning TEM at 300 kV.

dc magnetization was measured as a function of temperature using a Quantum Design Magnetic Property Measurement System. For a temperature sweep experiment, the sample was zero-field cooled (ZFC) to 1.8 K and data were collected by warming from 2 to 300 K in an applied field.

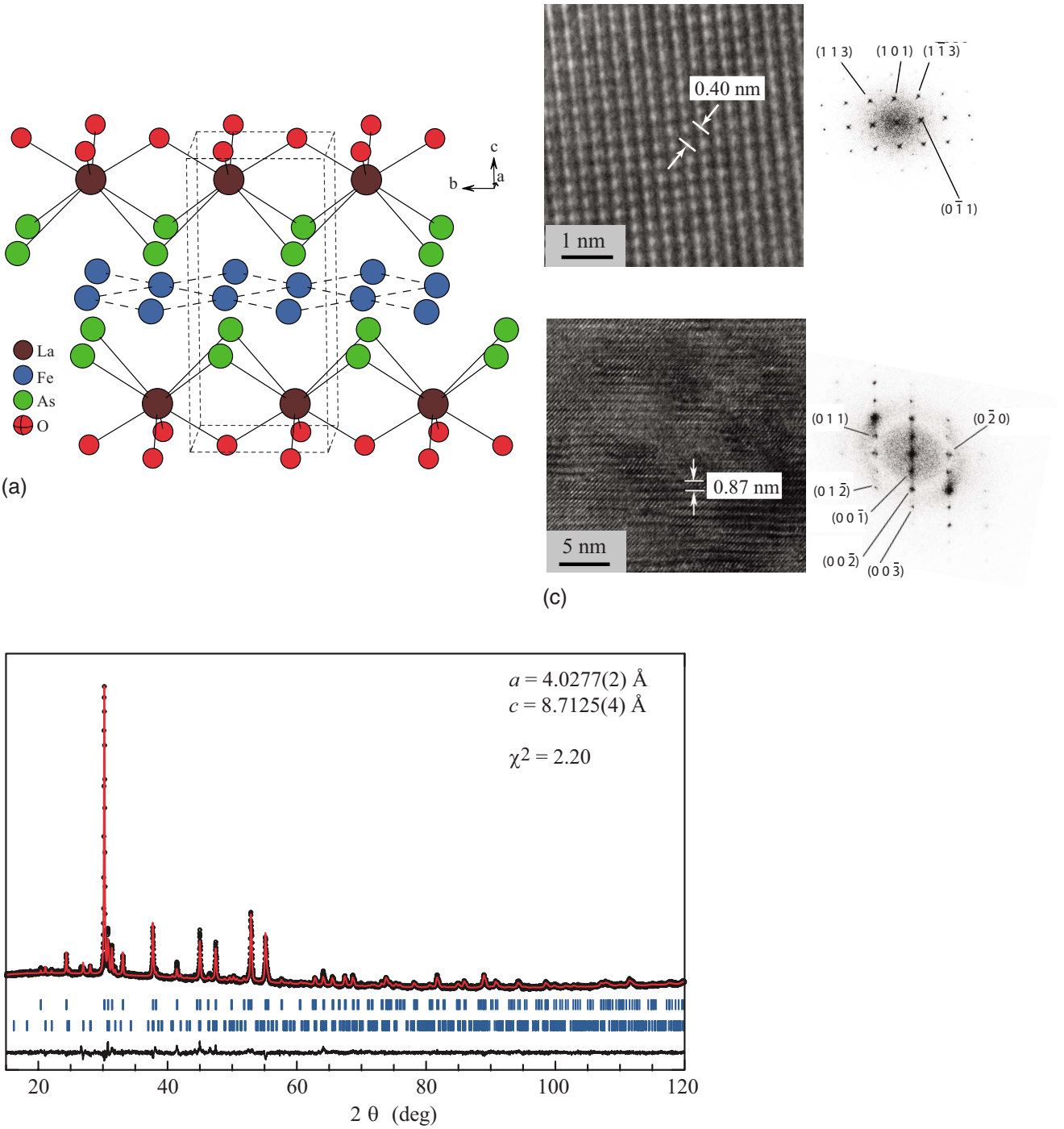

FIG. 1. (a) (Color online) Crystal structure of $LaFeAsO_{0.89}F_{0.11}$, with unit cell shown in dotted lines. The structure is made from layers of face-sharing distorted square antiprism of $LaAs_4O_4$ and sheets of Fe, perpendicular to the c direction. (b) The refined x-ray powder diffraction of nominal composition $LaFeAsO_{0.89}F_{0.11}$. The upper set of Bragg ticks correspond to reflections from this structure; the lower ticks locate reflections from ≈5% impurity phase of $La_{4.67}(SiO_4)_3O$. (c) TEM images and FFT calculated diffraction patterns for two crystallographic orientations of $LaFeAsO_{0.89}F_{0.11}$. The view along the c axis and that perpendicular to it are shown in the top and bottom panels, respectively. The lengths of a and c axes are labeled.

The sample was then field cooled (FC) in the applied field, and the measurement repeated from 1.8 K. The magnetic susceptibility results may be presented per mole of $LaFeAsO_{0.89}F_{0.11}$ f.u. (cm^3/mol).

Temperature-dependent electrical resistivity, thermal conductivity, and Seebeck coefficient measurements were obtained by using a Quantum Design Physical Property Measurement System (PPMS). For dc resistance measurements, electrical contacts were placed on samples in standard four-probe geometry by using Pt wires and silver epoxy (EPOTEK H20E). The Hall component was found from the Hall resistivity (ρ_{xy}) under magnetic field reversal at a given

temperature. For the thermal transport option, gold coated copper leads were used. For thermal transport option, typical $\Delta T/T$ values were about 5% at low temperatures ($T < 40$ K) and about 1% at higher temperatures. Specific heat data, $C_p(T)$, were also obtained using a PPMS via the relaxation method.

III. RESULTS AND DISCUSSION

A. Powder x-ray diffraction and microanalysis

Results of Rietveld refinement of the diffraction data are shown in Fig. 1(b). The overall agreement factors are $R_p = 1.36$ and $R_{wp} = 1.86$. The quality of the refinement is satisfactory, as indicated by the value of $\chi^2 = 2.20$. R_{Bragg} for the target phase is low (8.32), which indicates a good fit. For the secondary phase of $La_{4.67}(SiO_4)_3O$, the refinement was impeded by its small presence, complexity of the structure, and the overlap between strong peaks of the two phases giving $R_{Bragg} = 24.1$. However, excluding this phase reduces the quality of the overall refinement ($\chi^2 = 3.30$). Quantitative phase analysis was precluded by the poor refinement of the secondary phase. Inspection of a polished surface under optical microscope and SEM (described below) suggests ≈5% lanthanum silicate oxide. No evidence of inhomogeneous fluorine distribution is observed in the powder x-ray diffraction peaks.

The refined lattice constants of $LaFeAsO_{0.89}F_{0.11}$ are $a = 4.0277(2)$ Å and $c = 8.7125(4)$ Å, as shown in Fig. 1(b). These values compare well with that reported for 5% F-doped sample with $a = 4.0320(1)$ Å and $c = 8.7263(3)$ Å,[4] and smaller than the reported lattice constants of LaFeAsO with $a = 4.038(1)$ Å and $c = 8.753(6)$ Å.[7] As expected, the incorporation of F in place of O reduces the size of the unit cell. La and As are located at Wyckoff positions 2*c* with $z = 0.1455(3)$ and 0.6522(5), respectively. Fe is at 2*b* and the shared O/F site is at 2*a*. Nearest neighbor interatomic distances are d(La-O/F) = 2.380(1) Å, d(La-As) = 3.349(3) Å, and d(Fe-As) = 2.411(2) Å. Similar distances are reported for PrFeAsO.[7] The nearest neighbor Fe-Fe distance in $LaFeAsO_{0.89}F_{0.11}$ is 2.8481(1) Å.

Electron probe microanalysis and SEM are used to complement powder x-ray diffraction data for further investigation of sample purity. Standardless, semiquantitative analysis of energy-dispersive x-ray spectra confirm the presence of La, Fe, As, O, and F with La:Fe:As ≈ 1:1:1. Reliable estimates of the F content are precluded by the near exact overlap of the F *K* and Fe *L* lines in the microprobe data; however, the presence of F is suggested by the excess intensity of the line near Fe *L* and independently confirmed by x-ray photoelectron spectroscopy measurements. There is no fluorine-containing secondary phase observed in electron probe microanalysis, but there is the presence of small amounts of Fe_2As and the lanthanum silicate oxide impurity phases. No indication of Fe_2As is observed in the powder diffraction data, limiting the concentration of this impurity to less than a few percent. It is likely that the lanthanum silicate is formed by reaction with SiO vapor present in the silica tubes at the high temperatures of 1250 °C, at which the sample is formed. TEM images and fast Fourier transform (FFT) calculated diffraction patterns for two crystallographic orientations of $LaFeAsO_{0.89}F_{0.11}$ are shown in Fig. 1(c). The view along the *c* axis and that perpendicular to it are shown on top and bottom, respectively. The lengths of the *a* and *c* axes are labeled. The layered nature of the $LaFeAsO_{0.89}F_{0.11}$ structure is clearly visible.

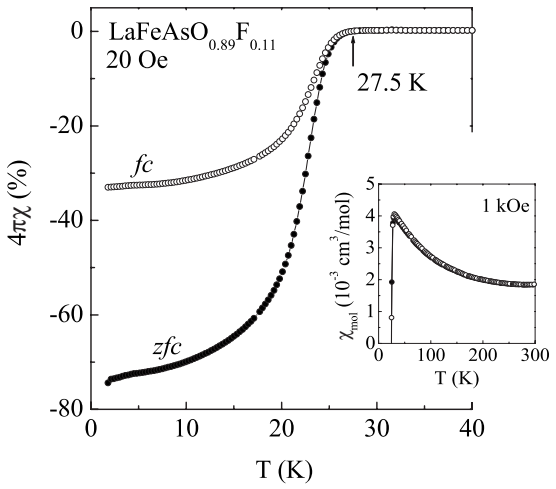

FIG. 2. Temperature dependence of the ZFC (filled circles) and FC (open circles) magnetic susceptibility for $LaFeAsO_{0.89}F_{0.11}$ in 20 and 1 kOe (inset).

B. Physical properties

Figure 2 shows the temperature dependence of the magnetic susceptibility χ measured under ZFC and FC conditions at 20 Oe. The susceptibility becomes negative below 27.5 K. The shielding fraction is given by the ZFC data and the Meissner fraction by the FC curve. Assuming theoretical density of 6.68 g/cm^3, a shielding fraction of 74% and a Meissner fraction of 33% are found at 2 K. The temperature dependence of susceptibility above T_c at 1 kOe is shown in the inset of Fig. 2. The magnetic susceptibility is similar to that reported by Kamihara *et al.*,[4] with χ varying from 1.8×10^{-3} cm^3/mol at room temperature to 4.1×10^{-3} cm^3/mol at 30 K, with M vs H curves linear in this temperature range. This value is approximately 50 times the expected bare susceptibility of $\chi_0 = 8.51 \times 10^{-5}$ cm^3/mol, which was recently found from density functional theory and local spin density approximation [L(S)DA].[8] Several different fluorine-doped LaFeAsO samples were synthesized by using different combinations of elements and binary phases, but the high-temperature susceptibility data from all of these samples were of similar magnitude to that shown in Fig. 2, inset. This suggests that the large value of the susceptibility may be intrinsic to the superconducting phase and not due to an impurity phase or inhomogeneous fluorine doping (see Sec. III A). This indicates that the superconductor may be close to magnetic ordering. Within the LDA, LaFeAsO is also reported to be on the borderline of a ferromagnetic instability.[8]

Figure 3(a) shows the temperature dependence of the electrical resistivity (ρ) in zero field. At room temperature, $\rho_{300\ K} = 2.7$ mΩ cm, which is comparable to the reported val-

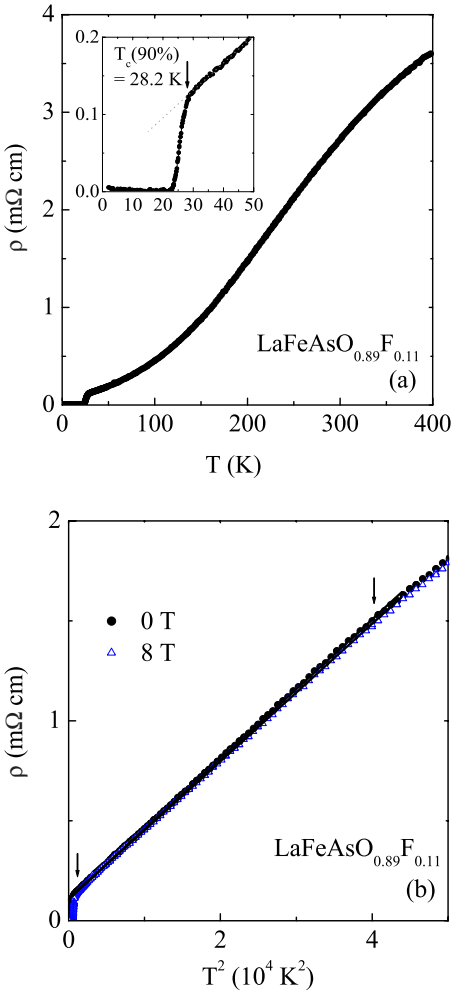

FIG. 3. (Color online) Temperature dependence of electrical resistivity for $LaFeAsO_{0.89}F_{0.11}$, which is shown as (a) ρ vs T and (b) ρ vs T^2 between 0 and ~225 K. The inset of (a) is the enlarged low-temperature data, with the indicated superconducting transition temperature. In (b), the red solid lines represent the linear fit between 35 and 200 K (shown by arrows) for data in 0 and 8 T.

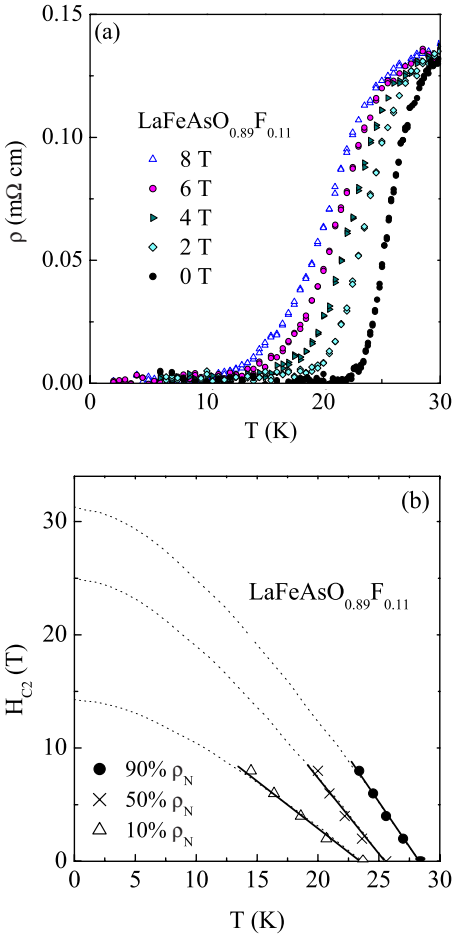

FIG. 4. (Color online) For $LaFeAsO_{0.89}F_{0.11}$, the temperature dependence of (a) resistivity at various applied fields and (b) the upper critical field H_{c2} found from 90%, 50%, and 10% of the normal-state value, ρ_N. In (b), the dotted lines represent the WHH approach and the solid lines are the linear fits to experimental $H_{c2}(T)$.

ues of 3.5 mΩ cm (Ref. 4) and 2.2 mΩ cm.[5] The inset is the enlarged view below 50 K with the onset transition temperature $T_c^{\text{onset}}=28.2$ K (using the 90% criterion) and a transition width $\Delta T_c=T_c(90\%)-T_c(10\%)=4.5$ K. In analyzing the resistivity data above T_c, we find that ρ exhibits a quadratic temperature dependence, $\rho=\rho_0+AT^2$, over a wide temperature range. Plotted in Fig. 3(b) is $\rho(T^2)$ for $H=0$ (open triangles) and $H=8$ T (filled circles) and linear fits between T_c and 200 K. The A values are 3.5×10^{-5} and 3.4×10^{-5} mΩ cm K^{-2} for $H=0$ and 8 T, respectively, and $\rho_0\approx0.11$ mΩ cm. The T^2 behavior of ρ below 200 K indicates the importance of the umklapp process of the electron-electron scattering and is consistent with the formation of a Fermi-liquid state. The A values extracted here are comparable with semiheavy-fermion compounds such as $CePd_3$ and UIn_3.[13]

Figure 4(a) illustrates that the resistive transition for $LaFeAsO_{0.89}F_{0.11}$ shifts to lower temperatures by applying a magnetic field. The transition width becomes wider with increasing H, which is a characteristic of type-II superconductivity. Here, we define a transition temperature $T_c(H)$ that satisfies the condition that $\rho(T_c,H)$ equals a fixed percentage of the normal-state value (ρ_N) for each field H. The $T_c(H)$ values for $\rho=10\%$, 50%, and 90% are shown in Fig. 4(b), which are represented by the upper critical field $H_{c2}(T)$. In all cases, we find that $H_{c2}(T)$ has a linear dependence with no sign of saturation. The slope $(dH_{c2}/dT)|_{T=T_c}=-0.87$ T/K for $\rho_N=10\%$, −1.41 T/K for $\rho_N=50\%$, and −1.59 T/K for $\rho_N=90\%$. In the conventional BCS picture, H_{c2} is linear in T near T_{c0} and saturates in the 0 K limit, however, deviations may be caused in the presence of impurity scattering.[14] In the latter case, Werthamer–Helfand–Hohenberg (WHH) equation is $H_{c2}(0)=-0.693T_c(dH_{c2}/dT)|_{T=T_c}$. The dashed lines in Fig. 4(b) are the results of fitting $H_{c2}(T)$ to the WHH formula, yielding $H_{c2}^{\text{WHH}}(0)=14.3$ T for $\rho_N=10\%$, 25.0 T for $\rho_N=50\%$, and 31.2 T for $\rho_N=90\%$. It should be noted that at lower temperatures, $H_{c2}(T)$ no longer follows the WHH expression, particularly for $\rho_N=10\%$, which suggests that $H_{c2}(0)$ is probably larger than $H_{c2}^{\text{WHH}}(0)$. In a recent publication, higher upper critical field of ~54 T was reported.[5] Nevertheless, assuming $H_{c2}(0)=H_{c2}^{\text{WHH}}(0)$, the Ginzburg–Landau

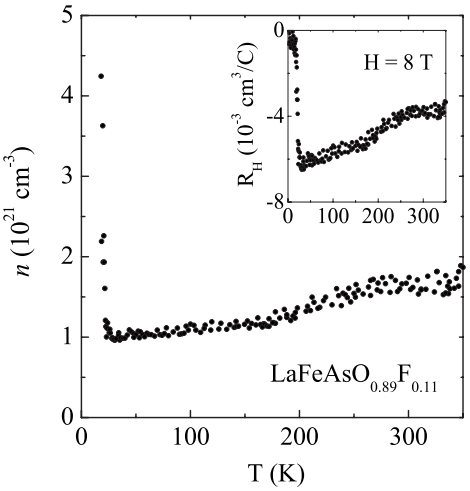

FIG. 5. The inferred variation of the carrier density n with temperature for $LaFeAsO_{0.89}F_{0.11}$. The inset is the temperature dependence of the Hall coefficient R_H obtained in a magnetic field of 8 T.

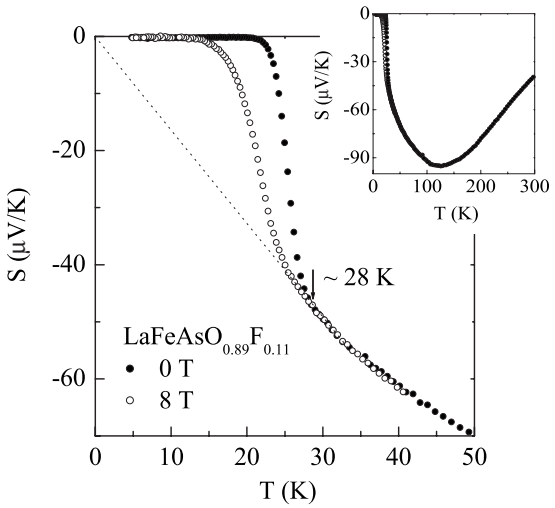

FIG. 6. Temperature dependence of Seebeck coefficient for $LaFeAsO_{0.89}F_{0.11}$ in applied fields of 0 and 8 T. The inset shows the temperature dependence up to room temperature. The dotted line is extrapolation from ~35 K down to 0.

formula is $\xi_{GL}=(\Phi_0/2\pi H_{c2})^{1/2}$, where $\Phi_0=2.07\times10^{-7}$ Oe cm^2. This yields zero temperature coherence length $\xi_{GL}(0)\approx48$ Å for $H_{c2}(10\%\rho_N)$, 36 Å for $H_{c2}(50\%\rho_N)$, and 33 Å for $H_{c2}(90\%\rho_N)$. These values are slightly larger than that reported (25 Å) (Ref. 5) and comparable to those for high-temperature superconducting cuprates with similar transition temperatures.[15–17]

The temperature-dependent specific heat for $LaFeAsO_{0.89}F_{0.11}$ has no observable anomaly near T_c. Although the large value of the lattice specific heat near T_c would make the superconducting contribution at T_c fairly small (of order 1–3 %), the lack of any anomaly above the precision of our data is somewhat surprising. We measured several different polycrystalline samples that showed relatively large Meissner fractions but were unable to detect any anomaly at T_c. The contribution of electronic value is $\gamma=1.0(3)$ mJ/K^2 mol atom [4.1(1) mJ/K^2 mol] from C/T vs T^2 plot and the straight line for the region of ~4–8 K. This γ value may not be intrinsic to the superconducting phase; this is perhaps due to metallic Fe_2As found in microprobe analysis. From high-temperature data, the Debye temperature is $\theta_D\approx325$ K; this value is comparable to that recently derived from specific heat results ($\theta_D=315.7$ K).[10]

Figure 5 shows the results of temperature-dependent Hall data. The Hall coefficient (Fig. 5, inset) is negative and gradually decreases with decreasing temperature down to ~130 K below which it is approximately constant. If a single band is assumed, the inferred carrier concentration is $\approx1.7\times10^{21}$ electrons/cm^3 at room temperature and $\approx1\times10^{21}$ electrons/cm^3 just above T_c. Our Hall data are similar to those recently reported.[9] The electronic structure calculations[8] also predict a similar carrier concentration, as well as the presence of both high velocity electron bands and heavy hole bands near the Fermi energy, with the electron bands dominating in-plane transport. Because of the possibility of some electrical conduction by holes, the low-temperature carrier concentration of 1×10^{21} electrons/cm^3 should be regarded as an upper bound for the electron carrier concentration just above T_c.

The Seebeck coefficient of $LaFeAsO_{0.89}F_{0.11}$, S, is shown in Fig. 6. S is negative and large, varying from −42 μV/K at 300 K to a maximum negative value of ~−95 μV/K at ~130 K, then decreasing toward 0. The maximum in the Seebeck coefficient and the slight temperature dependence of the Hall data are probably due to the competition between dominant electronlike bands and the expected proximity of holelike bands near the Fermi energy.

The low-temperature Hall data and Seebeck coefficient (Figs. 5 and 6) can be used to obtain a qualitative estimate of the effective mass of the carriers m^* and the Sommerfeld coefficient γ. If we assume that the electron carrier concentration below ~130 K is close to the value inferred from the Hall data (1×10^{21} electrons/cm^3), the free electron model predicts a Fermi energy (temperature) of 0.4 eV (4800 K).[19] The Seebeck coefficient at 40 K is −60 μV/K and in the temperature regime, roughly extrapolates linearly to 0 at $T=0$ (Fig. 6). In many normal low carrier concentration metals,[18] the Seebeck coefficient is given by the diffusion contribution of the Mott expression or $S=\pi^2k_BT(2eT_F)^{-1}$, where T_F is the Fermi temperature. If we use a value for of 4800 K for T_F in the expression for S, this results in a Seebeck value of ≈−3.5 μV/K at 40 K, which is much smaller than the measured value of −60 μV/K. These results imply a value for $m^*\approx17$ and a corresponding value of $\gamma\approx11$ mJ/K^2 mol,[19] which is about twice the calculated density of states at E_f ($\gamma_0=6.5$ mJ/K^2 mol).[8] Although this is clearly a crude estimate, it suggests that electronic correlations are important in $LaFeAsO_{0.89}F_{0.11}$, as were suggested from $\rho(T^2)$ analyses above. We also note that the value of $\gamma=4.1(1)$ mJ/K^2 mol extracted from the specific heat data may reflect that a portion of the $LaFeAsO_{0.89}F_{0.11}$ phase remains in the normal state.

For $LaFeAsO_{0.89}F_{0.11}$, the temperature-dependent thermal conductivity is displayed in Fig. 7. An anomaly at ≈28 K is clearly evident. Because of the low carrier concentration and high resistivity, most of the heat in this compound is carried

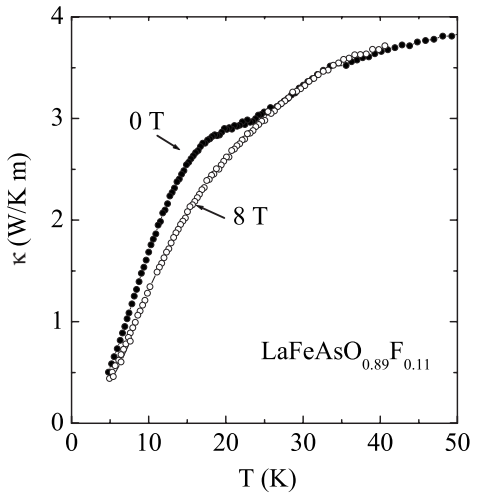

FIG. 7. Temperature dependence of thermal conductivity data for $LaFeAsO_{0.89}F_{0.11}$ in applied fields of 0 and 8 T.

by phonons. Above T_c, approximately 85% of the heat is carried by phonons, as estimated using the Wiedemann–Franz relationship. Just below T_c, the electrons that condense into the superconducting state should carry no heat because of the opening of the superconducting gap. Since electrons that carry heat are removed below T_c, one would expect that the thermal conductivity should decrease below T_c, as occurs in most superconductors.[20–22] The opposite occurs in $LaFeAsO_{0.89}F_{0.11}$ below T_c, as the thermal conductivity is *higher* than the expected normal-state values. This is clear from a comparison of the 0 field data with thermal conductivity data taken at 8 T that suppresses T_c by about 5 K (Fig. 7). Similar behavior is observed in the cuprate superconductors.[23,24] One explanation for the higher value of κ for $LaFeAsO_{0.89}F_{0.11}$ just below T_c, which is consistent with the evidence for strong electron-electron scattering, is an increase in the mobility of the fraction of electrons still in the normal state.

IV. CONCLUSIONS

The crystal structure, magnetic susceptibility, specific heat, resistivity, Hall effect, Seebeck coefficient, and thermal conductivity of the layered $LaFeAsO_{0.89}F_{0.11}$ superconductor were investigated in this paper. The magnetic susceptibility clearly indicates bulk superconductivity with Meissner fraction of ≈30% and screening fraction of ≈70%. Analysis of the resistivity, Seebeck coefficient, thermal conductivity, and high-temperature magnetic susceptibility data suggest that electron-electron correlations are large in this compound. The relationship between correlations and superconductivity will require further experimental investigations by using single crystals as well as substantial insight from theoretical calculations.

ACKNOWLEDGMENTS

We would like to thank D. J. Singh for helpful discussions, H. M. Meyer for x-ray photoemission spectroscopy analyses, and G. M. Veith for assistance with SEM and x-ray diffraction data collections. Research sponsored by the Division of Materials Science and Engineering, Office of Basic Energy Sciences. Oak Ridge National Laboratory is managed by UT-Battelle, LLC, for the U.S. Department of Energy under Contract No. DE-AC05-00OR22725.

[1] Y. Kamihara, H. Hiramatsu, M. Hirano, R. Kawamura, H. Yanagi, T. Kamiya, and H. Hosono, J. Am. Chem. Soc. **128**, 10012 (2006).
[2] C. Y. Liang, R. C. Che, H. X. Yang, H. F. Tian, R. J. Xiao, J. B. Lu, R. Li, and J. Q. Li, Supercond. Sci. Technol. **20**, 687 (2007).
[3] T. Watanabe, H. Yanagi, T. Kamiya, Y. Kamihara, H. Hiramatsu, M. Hirano, and H. Hosono, Inorg. Chem. **46**, 7719 (2007).
[4] Y. Kamihara, T. Watanabe, M. Hirano, and H. Hosono, J. Am. Chem. Soc. **30**, 3296 (2008).
[5] V. Johnson and W. Jeitschko, J. Solid State Chem. **11**, 161 (1974).
[6] B. I. Zimmer, W. Jeitschko, J. H. Albering, R. Glaum, and M. Reehuis, J. Alloys Compd. **229**, 238 (1995).
[7] P. Quebe, L. J. Terbüchte, and W. Jeitschko, J. Alloys Compd. **302**, 70 (2000).
[8] D. J. Singh and M. H. Du, arXiv:0803.0429 (unpublished).
[9] G. F. Chen, Z. Li, G. Li, J. Zhou, D. Wu, J. Dong, W. Z. Hu, P. Zheng, Z. J. Chen, J. L. Luo, and N. L. Wang, arXiv:0803.0128 (unpublished).
[10] G. Mu, X. Zhu, L. Fang, L. Shan, C. Ren, and H. Wen, arXiv:0803.0928 (unpublished).
[11] J. Rodriguez-Carvajal, FULLPROF suite, Version 3.30, ILL, June 2005.
[12] E. A. Kuz'min and A. N. V. Belov, Dokl. Akad. Nauk SSSR **165**, 88 (1965).
[13] K. Kadowaki and S. B. Woods, Solid State Commun. **58**, 507 (1986).
[14] S. Maekawa, H. Ebisawa, and H. Fukuyama, J. Phys. Soc. Jpn. **52**, 1352 (1983).
[15] M. Suzuki and M. Hikita, Phys. Rev. B **44**, 249 (1991).
[16] E. M. Motoyama, G. Yu, I. M. Vishik, O. P. Vajk, P. K. Mang, and M. Greven, Nature (London) **445**, 186 (2007).
[17] Y. Wang, S. Ono, Y. Onose, G. Gu, Y. Ando, Y. Tokura, S. Uchida, and N. P. Ong, Science **299**, 86 (2003).
[18] J. McCarten, S. E. Brown, C. L. Seaman, and M. B. Maple, Phys. Rev. B **49**, 6400 (1994).
[19] C. Kittel, *Introduction to Solid State Physics*, 3rd ed. (Wiley, New York, 1986), Chap. 7.
[20] J. E. Smith and D. M. Ginsberg, Phys. Rev. **167**, 345 (1968).
[21] C. Gladun, H. Madge, and H. Vinzelberg, Phys. Status Solidi A **62**, 503 (2006).
[22] S. D. Peacor, R. A. Richardson, J. Burm, and C. Uher, Phys. Rev. B **42**, 2684 (1990).
[23] K. Krishana, N. P. Ong, Q. Li, G. D. Gu, and N. Koshizuka, Science **277**, 83 (1997).
[24] C. Uher and W.-N. Huang, Phys. Rev. B **40**, 2694 (1989).